

Phase-dependence correlated electron momentum distribution from nonsequential double ionization of N₂ by few-cycle laser pulses

Yueming ZHOU, Peixiang LU (✉)

Wuhan National Laboratory for Optoelectronics, Huazhong University of Science and Technology, Wuhan 430074, China

© Higher Education Press and Springer-Verlag Berlin Heidelberg 2010

Abstract Using the classical three-dimensional (3D) ensembles, we have investigated nonsequential double ionization (NSDI) of N₂ by phase-stabilized few-cycle pulses. We find that the correlated electron momentum distributions in the direction parallel to the laser field strongly depend on the carrier-envelope phase (CEP) of few-cycle pulses, and this phase dependence is not affected by the alignment of the molecular axis relative to the laser field. Back analysis reveals that the ionization rate of the first electron and the recollision energy play a main role in the electron momentum distributions. Our results suggest that the few-cycle pulses with stabilized phase can serve as a powerful tool to investigate the recollision dynamics in NSDI of molecules.

Keywords nonsequential double ionization (NSDI), alignment, few-cycle, carrier-envelope phase (CEP)

1 Introduction

Nonsequential double ionization (NSDI) has been a hot topic in the strong field atomic and molecular physics because it reveals a highly correlated electron behavior. This behavior has provided profound insights into the physical mechanism of NSDI [1–8]. Nowadays, the widely accepted picture for NSDI is the quasiclassical recollision model [9], in which the first electron is tunneled through the suppressed potential barrier around the peak of the electric field. Then it is driven by the oscillating field and returns to the parent ion as the electric field reverses its direction, recolliding with the ion inelastically and leading to the second electron released directly in an (e, 2e) process or excited plus subsequential field ionization [10].

Recent advance in femtosecond laser technology has opened the door for studying laser-matter interaction on the time scale of a few optical cycles [11]. For such few-cycle pulses, the electric field $E(t) = E_0(t)\cos(\omega t + \varphi)$ depends on the phase of the carrier wave with respect to the pulse envelope $E_0(t)$ and the so-called carrier-envelope phase (CEP) φ . Recent experiments have shown that the high harmonic generation [12] and the left-right symmetry of the electron yields from above-threshold ionization [13] depend on the CEP of few-cycle pulses. For NSDI of atoms, experimental and theoretical studies have reported that the doubly charged ion momentum spectra are also significantly influenced by the CEP of few-cycle pulses [14–16]. For molecular targets, it has been reported that the NSDI yield of D₂ molecules also depends on the CEP of few-cycle pulses [17].

In this paper, with the classical three-dimensional (3D) ensemble model [18–20], we investigate NSDI of N₂ molecules by few-cycle pulses. We find that the correlated electron momentum distributions depend strongly on the CEP of the few-cycle pulses, and this phase dependence of the momentum distribution is not affected by the alignment of the molecular axis relative to the laser field. Back analysis reveals that the ionization rate of the first electron and its returning energy influence the correlated electron momentum distributions. Our results suggest that the few-cycle pulses with stabilized phase can serve as a powerful tool to investigate the recollision dynamics in NSDI of molecules.

2 Model

The 3D classical ensemble model has been successful in understanding of NSDI before, and it has been described detailedly in Refs. [18–20]. In this classical model, the evolution of the electron pairs is determined by the

Newton's motion equations (atomic units are used throughout this paper until stated otherwise) as

$$\frac{d^2 r_i}{dt^2} = -\nabla(V_{ne}^i + V_{ee}) - E(t), \quad (1)$$

where the index i denotes the two different electrons.

$$V_{ne}^i = -\frac{1}{\sqrt{(r_i - R/2)^2 + a^2}} - \frac{1}{\sqrt{(r_i + R/2)^2 + a^2}}$$

and

$$V_{ee} = \frac{1}{\sqrt{(r_1 - r_2)^2 + b^2}}$$

are the ion-electron and electron-electron interactions, respectively. $E(t)$ is the electric field, which can be written as

$$E(t) = E_0 \sin^2\left(\frac{t}{NT}\pi\right) \cos\left[\omega\left(t - \frac{NT}{2}\right) + \varphi\right] \hat{z}.$$

\hat{z} is the polarization vector. E_0 , T , ω , and φ are the amplitude, period, frequency, and CEP of the laser field, respectively. The intensity of the laser field is 2.0×10^{14} W/cm², and the wavelength is 800 nm. The pulse contains four optical cycles, i.e., $N=4$.

In our calculation, the two nuclei are fixed at $(0, \sin\theta, \cos\theta)$ and $(0, -\sin\theta, -\cos\theta)$, respectively, where θ is the angle between the molecular axis and the z axis. Thus, the internuclear vector is $R = (0, 2\sin\theta, 2\cos\theta)$. The initial energy of the ensemble is set to be the sum of the first and second ionization potentials of N₂, i.e., -1.7 a.u. To obtain the initial value, the ensemble is populated starting from a classically allowed position for the energy of -1.7 a.u. The available kinetic energy is distributed between the two electrons randomly in momentum space. Each electron is

given radial velocity only, with sign randomly selected. Then the electrons are allowed to evolve a sufficiently long time (100 a.u.) in the absence of the laser field to obtain stable position and momentum distributions. To avoid autoionization, the screening parameter a is set to be 1.00. Similar to Ref. [18], b is set to be 0.05. Figures 1(a) and 1(b) show the position distributions of the initial ensemble along the x and z axes, respectively, when the molecular axis is parallel to the z axis. Once the initial state is obtained, the laser field is turned on, and all the trajectories are evolved in the combined Coulomb and laser field. Double ionization (DI) is determined if both electrons achieve positive energies when the laser field is turned off.

3 Results and discussion

Figure 2 shows the correlated electron momentum distributions in the direction parallel to the laser field as a function of the CEP. For Figs. 2(a) and 2(b), the molecular axis is parallel to the laser polarization (i.e., $\theta=0^\circ$), while for Figs. 2(c) and 2(d), it is perpendicular to the laser polarization (i.e., $\theta=90^\circ$). It is clearly seen that most of the electrons are distributed in the first and third quadrants, which implies that $(e, 2e)$ pathway dominates the DI events in the few-cycle pulses. The correlated patterns in the first and third quadrants are obviously asymmetric with respect to the diagonal $K_1 = -K_2$ (K_1 and K_2 donate the momenta of the two electrons). When the molecular axis is parallel to the laser field and for $\varphi=0^\circ$, the yield from the third quadrant is higher than that from the first quadrant, while for $\varphi=90^\circ$, the yield from the first quadrant is much higher. When the molecular axis is perpendicular to the laser field, the total DI yield is much lower than that from the parallel molecules, which is consistent with previous studies [20,21]. However, the asymmetry of the correlated patterns is similar to that of the

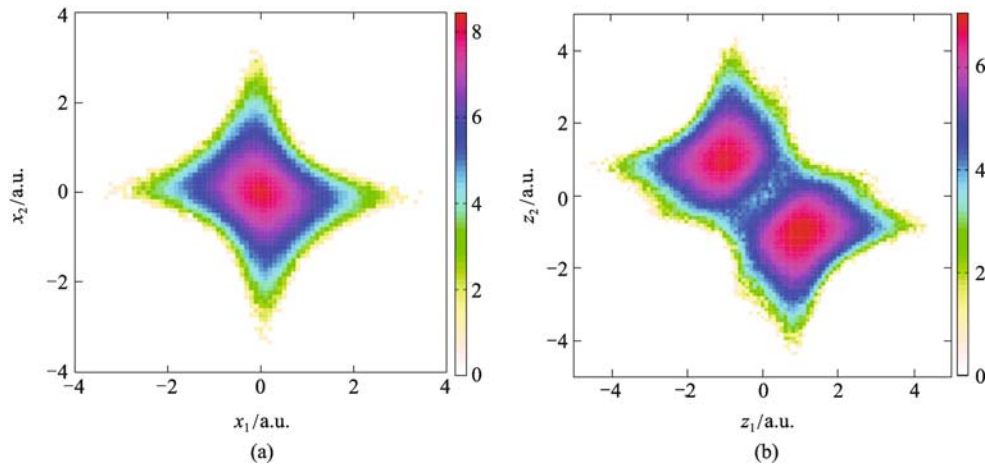


Fig. 1 Log plot of position distributions of initial ensemble when molecular axis is parallel to z axis (ensemble size is 5×10^5). (a) Along x axis; (b) along z axis

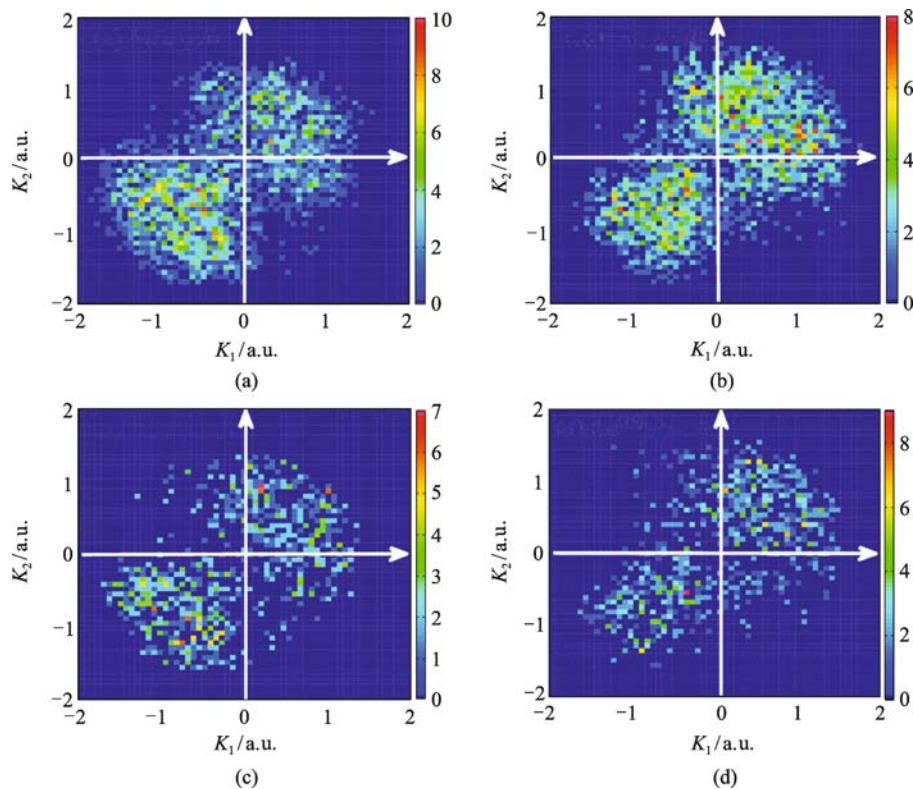


Fig. 2 Correlated electron momentum distribution. (a) $\varphi=0^\circ$, molecular axis is parallel to laser field, ensemble sizes are 0.5×10^6 , and about 2500 DI trajectories are obtained; (b) $\varphi=90^\circ$, molecular axis is parallel to laser field, ensemble sizes are 0.5×10^6 , and about 2500 DI trajectories are obtained; (c) $\varphi=0^\circ$, molecular axis is perpendicular to laser field, ensemble sizes are 1.5×10^6 , and about 1000 DI trajectories are obtained; (d) $\varphi=90^\circ$, molecular axis is perpendicular to laser field, ensemble sizes are 1.5×10^6 , and about 1000 DI trajectories are obtained

parallel molecules. It implies that the phase dependence of the correlated electron momentum distribution is not obviously affected by the molecular alignment.

To understand the detailed dynamics of molecular NSDI by the few-cycle pulses, we take advantage of back analysis. We defined that an electron is ionized if its energy is greater than zero. The recollision time is defined to be the instant of the closest approach of the two electrons after the first departure of one electron from the core, and the DI time is defined to be the instant when both electrons achieve positive energies, where the energy contains the kinetic energy, ion-electron interaction and half electron-electron repulsion. Figure 3 shows the counts of the DI trajectories from Figs. 2(a) and 2(b) versus the ionization time of the first electron, the recollision time and the DI time. For $\varphi=0^\circ$, the first electrons are ionized around P_1 and P_2 (as indicated in Fig. 2(a)). The count of the trajectories where the first ionization occurs around P_1 is larger than that around P_2 , even though the electric field at P_2 is stronger than that at P_1 . This is due to the fact that a great part of the electrons ionized around P_2 cannot be driven back to the parent ion with sufficient energy to release the second electrons. For $\varphi=90^\circ$, because of the weak electric field at P_1 , the ionization probability of the

first electron around P_1 is much lower than that around P_2 .

The electron ionized around an extremum of the electric field is driven back to the parent ion about $2/3$ optical cycle later. As shown in Figs. 3(c) and 3(d), the electrons ionized around P_1 and P_2 return to the parent ions at t_1 and t_2 , respectively. Assuming the electric field to be a plane wave $E_0 \cos(\omega t + \varphi)$, the electron's final momentum is determined by $v_0 + E_0 \sin(\omega t_i + \varphi)/\omega$, where t_i is the ionization time, and v_0 is the velocity at t_i . Because the electron gives up a sizable part of its energy in recollision, v_0 is often negligible comparing with $E_0 \sin(\omega t_i + \varphi)/\omega$. Thus, the direction of the electron's final momentum is determined by the latter of the terms. As will be addressed below, for the intensity we used, most of the second electrons are immediately ionized after recollision. Thus, the trajectories where the first ionization occurs around P_1 contribute to the yield in the third quadrant, and those where the first ionization occurs around P_2 contribute to the yield in the first quadrant.

From Fig. 2(b), we can find that the region of the momentum distribution in the first quadrant is wider than that in the third quadrant. It is well known that in the (e, 2e) process, the correlated electron momentum is distributed in a circle centered at $-A(t_i)$ with radius $\sqrt{2E_{\text{exc}}}$ [10], where

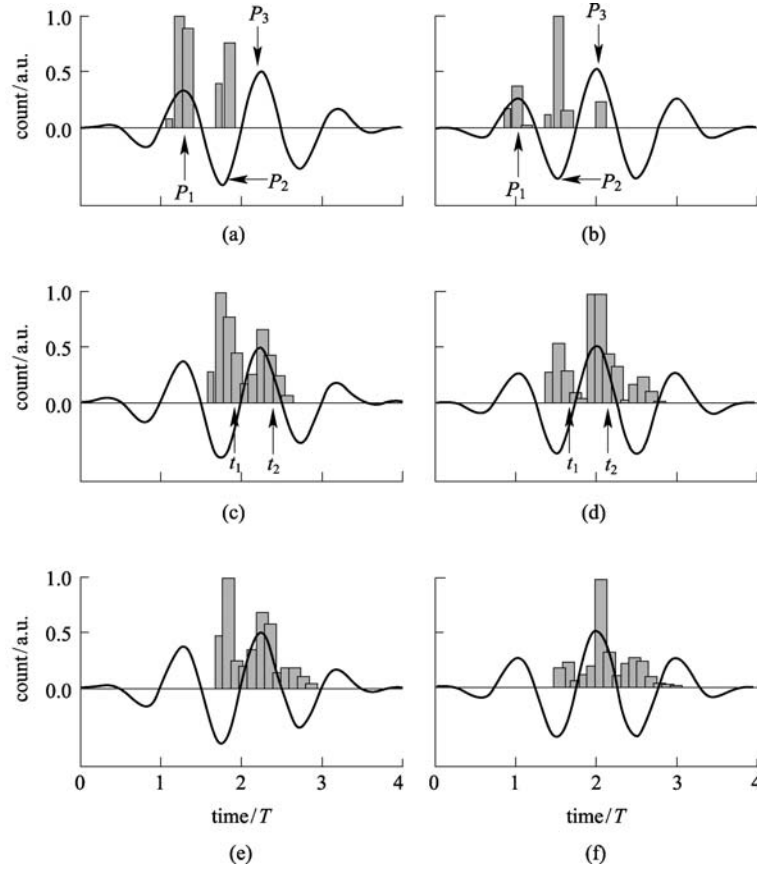


Fig. 3 (a) Count of DI trajectories versus ionization time of the first electron, CEP is 0° ; (b) count of DI trajectories versus ionization time of the first electron, CEP is 90° ; (c) count of DI trajectories versus recollision time, CEP is 0° ; (d) count of DI trajectories versus recollision time, CEP is 90° ; (e) count of DI trajectories versus DI time, CEP is 0° ; (f) count of DI trajectories versus DI time, CEP is 90° (arrows in (a) and (b) indicate the peaks of electric field)

$$A(t_i) = - \int_{-\infty}^{t_i} E(t) dt$$

is the vector potential, and E_{exc} is the excess energy of the recolliding electron. In Figs. 4(a) and 4(b), we show the time delay between recollision and DI for the trajectories from Figs. 2(a) and 2(b), respectively. The solid curves indicate the trajectories from the first quadrants, and the dashed curves indicate those from the third quadrants. It clearly shows that most of the DI occurs within 1/5 cycle of recollision, which implies that (e, 2e) process dominates the DI trajectories. In Figs. 5(a) and 5(b), we display the recollision energy of the returning electrons from Figs. 2(a) and 2(b), respectively. For $\varphi = 0^\circ$, the recollision energies of trajectories from the first and the third quadrants are similar, while for $\varphi = 90^\circ$, the recollision energies of the trajectories from the first quadrant are much higher than those from the third quadrant, and thus, the excess energies are larger. As a consequence, the momentum distribution

region for the trajectories in the first quadrant is wider than that in the third quadrant.

4 Conclusion

In conclusion, we have investigated the correlated electron momentum distribution of molecular NSDI in the intense few-cycle pulses with a classical ensemble model. The correlated electron momentum distributions strongly depend on the CEP of the few-cycle pulses, and this CEP dependence is not influenced by the alignment of the molecular axis relative to the laser polarization direction. Back analysis reveals that the ionization rate and the recollision energies of the first electrons affect the momentum distributions. Our results suggest that the subcycle dynamics of molecular NSDI can be controlled by varying the CEP of the few-cycle pulses.

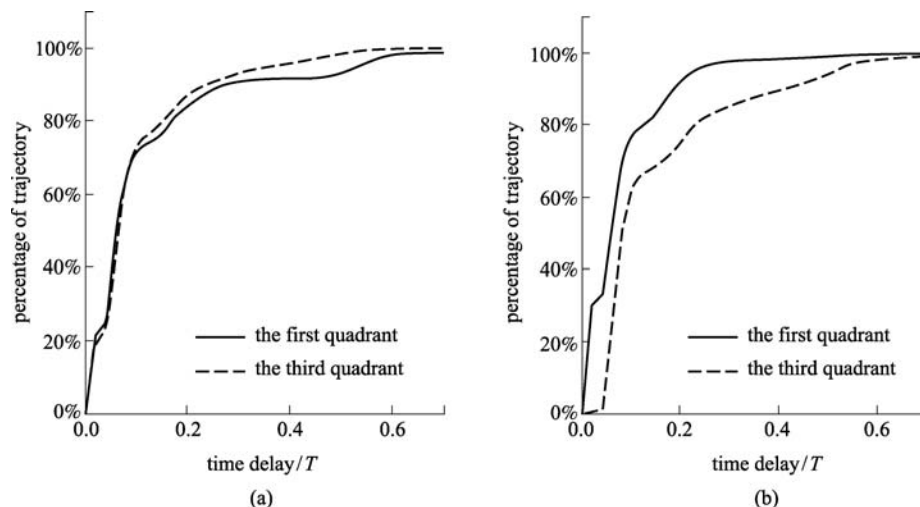


Fig. 4 Accumulated fraction of DI versus time delay between recollision and DI for trajectories. (a) From Fig. 2(a) while $\varphi=0^\circ$; (b) from Fig. 2(b) while $\varphi=90^\circ$ (solid curves indicate trajectories from the first quadrants, and dashed curves indicate trajectories from the third quadrants)

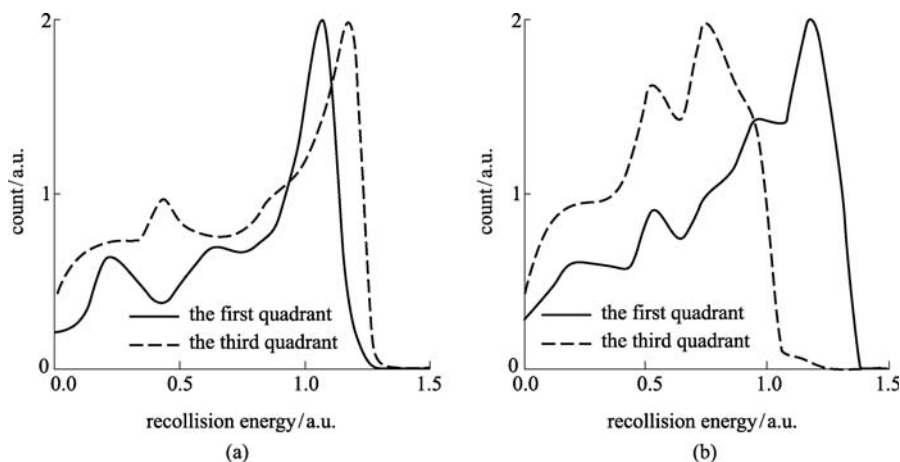


Fig. 5 Counts of trajectories versus recollision energy of the first electron for trajectories. (a) From Fig. 2(a) while $\varphi=0^\circ$; (b) from Fig. 2(b) while $\varphi=90^\circ$ (solid curves indicate trajectories from the first quadrants, and dashed curves indicate trajectories from the third quadrants)

Acknowledgements This work was supported by the National Natural Science Foundation of China (Grant No. 10774054), the National Science Fund for Distinguished Young Scholars (No. 60925021), and the National High Technology Research and Development Program of China (No. 2006CB806006).

References

1. Weber Th, Giessen H, Weckenbrock M, Urbasch G, Staudte A, Spielberger L, Jagutzki O, Mergel V, Vollmer M, Dörner R. Correlated electron emission in multiphoton double ionization. *Nature*, 2000, 405(6787): 658–661
2. Moshhammer R, Feuerstein B, Schmitt W, Dorn A, Schröter C D, Ullrich J, Rottke H, Trump C, Wittmann M, Korn G, Hoffmann K, Sandner W. Momentum distributions of Ne^{n+} ions created by an intense ultrashort laser pulse. *Physical Review Letters*, 2000, 84(3): 447–450
3. Chaloupka J L, Rudati J, Lafon R, Agostini P, Kulander K C, Dimauto L F. Observation of a transition in the dynamics of strong-field double ionization. *Physical Review Letters*, 2003, 90(3): 033002
4. Rudenko A, Zrost K, Feuerstein B, de Jesus V L B, Schröter C D, Moshhammer R, Ullrich J. Correlated multielectron dynamics in ultrafast laser pulse interactions with atoms. *Physical Review Letters*, 2004, 93(25): 253001
5. Staudte A, Ruiz C, Schöffler M, Schössler S, Zeidler D, Weber Th, Meckel M, Villeneuve D M, Corkum P B, Becker A, Dörner R. Binary and recoil collisions in strong field double ionization of helium. *Physical Review Letters*, 2007, 99(26): 263002
6. Rudenko A, de Jesus V L B, Ergler Th, Zrost K, Feuerstein B,

- Schröter C D, Moshhammer R, Ullrich J. Correlated two-electron momentum spectra for strong-field nonsequential double ionization of He at 800 nm. *Physical Review Letters*, 2007, 99(26): 263003
7. Liu Y, Tschuch S, Rudenko A, Dürr M, Siegel M, Morgner U, Moshhammer R, Ullrich J. Strong-field double ionization of Ar below the recollision threshold. *Physical Review Letters*, 2008, 101(5): 053001
 8. Fu L, Liu J, Chen J, Chen S. Classical collisional trajectories as the source of strong-field double ionization of helium in the knee regime. *Physical Review A*, 2001, 63(4): 043416
 9. Corkum P B. Plasma perspective on strong-field multiphoton ionization. *Physical Review Letters*, 1993, 71(13): 1994–1997
 10. Feuerstein B, Moshhammer R, Fischer D, Dorn A, Schröter C D, Deipenwisch J, Crespo Lopez-Urrutia J R, Höhr C, Neumayer P, Ullrich J, Rottke H, Trump C, Wittmann M, Korn G, Sandner W. Separation of recollision mechanisms in nonsequential strong field double ionization of Ar: the role of excitation tunneling. *Physical Review Letters*, 2001, 87(4): 043003
 11. Brabec T, Krausz F. Intense few-cycle laser fields: frontiers of nonlinear optics. *Reviews of Modern Physics*, 2000, 72(2): 545–591
 12. Baltuška A, Udem Th, Uiberacker M, Hentschel M, Goulielmakis E, Gohle Ch, Holzwarth R, Yakovlev V S, Scrinzi A, Hänsch T W, Krausz F. Attosecond control of electronic processes by intense light fields. *Nature*, 2003, 421(6923): 611–615
 13. Paulus G G, Grasbon F, Walther H, Villoresi P, Nisoli M, Stagira S, Priori E, De Silvestri S. Absolute-phase phenomena in photoionization with few-cycle laser pulses. *Nature*, 2001, 414 (6860): 182–184
 14. Liu X, Rottke H, Eremina E, Sandner W, Goulielmakis E, Keeffe K O, Lezius M, Krausz F, Lindner F, Schätzel M G, Paulus G G, Walther H. Nonsequential double ionization at the single-optical-cycle limit. *Physical Review Letters*, 2004, 93(26): 263001
 15. Zhou Y M, Liao Q, Lan P F, Lu P X. Classical effects of carrier-envelope phase on nonsequential double ionization. *Chinese Physics Letters*, 2008, 25(11): 3950–3953
 16. Liao Q, Lu P X, Zhang Q B, Hong W Y, Yang Z Y. Phase-dependent nonsequential double ionization by few-cycle laser pulses. *Journal of Physics B*, 2008, 41(12): 125601
 17. Tong X M, Lin C D. Carrier-envelope phase dependence of nonsequential double ionization of H₂ by few-cycle laser pulses. *Journal of Physics B*, 2007, 40(3): 641–649
 18. Haan S L, Breen L, Karim A, Eberly J H. Variable time lag and backward ejection in full-dimensional analysis of strong-field double ionization. *Physical Review Letters*, 2006, 97(10): 103008
 19. Zhou Y M, Liao Q, Lu P X. Mechanism for high-energy electrons in nonsequential double ionization below the recollision-excitation threshold. *Physical Review A*, 2009, 80(2): 023412
 20. Liao Q, Lu P X. Manipulating nonsequential double ionization via alignment of asymmetric molecules. *Optics Express*, 2009, 17(18): 15550–15557
 21. Liu J, Ye D F, Chen J, Liu X. Complex dynamics of correlated electrons in molecular double ionization by an ultrashort intense laser pulse. *Physical Review Letters*, 2007, 99(1): 013003